CHAPTER V
ROOM TEMPERATURE SYNTHESIS OF Ti-SBA-15 FROM SILATRANE AND TITANIUM-GLYCOLATE AND ITS CATALYTIC PERFORMANCE TOWARDS STYRENE EPOXIDATION

5.1 Abstract

A novel room temperature sol-gel synthesis of Ti-SBA-15 is described using moisture stable silatrane and titanium-glycolate precursors, and a non-ionic triblock copolymer ($EO_{20}PO_{70}EO_{20}$) as the structure directing agent. Catalyst performance was optimized by systematically investigating the influence of acidity, reaction time and temperature, and titanium loading. Small angle X-ray scattering (SAXS) and transmission electron microscopy (TEM) showed well-ordered 2D mesoporous hexagonal structures, while N_2 adsorption/desorption measurements yielded high surface areas (up to 670 m^2/g), with large pore diameters (5.79 nm) and volumes (0.83 cm^3/g). Diffuse reflectance UV-visible spectroscopy (DRUV) was found that tetravalent titanium as $Ti^{4+}O_4$ tetrahedra were incorporated in the framework through displacement of $Si^{4+}O_4$ after calcination (550 °C/6 h) to loadings of 7mol% Ti without perturbation of the ordered mesoporous structure, or decoration by extra-framework anatase containing $Ti^{4+}O_6$ octahedra. The catalytic activity and selectivity of styrene epoxidation using hydrogen peroxide (H_2O_2) showed that the conversion of styrene increases significantly at higher titanium contents. The only products of this reaction were styrene oxide and benzaldehyde, with selectivity of 34.2% and 65.8%, respectively, at a styrene conversion of 25.8% over the 7mol% Ti-SBA-15 catalyst. Beyond this titanium loading, anatase is deposited on the framework and catalytic activity degrades. The performance of the new catalyst is also shown to be superior to conventional materials produced by incipient wetness impregnation where Ti resides on the surface of SBA-15, giving a styrene conversion of 11.9% under identical reaction conditions.

(**Keywords**: Ti-SBA-15, silatrane, titanium-glycolate, styrene epoxidation)

5.2 Introduction

Since the discovery of the large and uniform hexagonal channel motifs, high specific surface area, and excellent hydrothermal stability of SBA-15 silica molecular sieve by Zhao *et al.* [1, 2], using nonionic triblock copolymers as templates, much effort has been devoted to enhancing the syntheses and functionality of these materials because of their potential as catalysts, adsorbents for large organic molecules, and guest-host chemical supports [3, 4]. However, pure silica porous materials are poor catalysts due to weak acidity and redox potential [5, 6]. To overcome these limitations, heteroatoms are incorporated into the framework to the create active sites, and many transition metals promote beneficial catalytic responses [7-10].

The introduction of Ti-substituted molecular sieves has added a new dimension to the application of silica based meso-frameworks for catalytic oxidation, and Ti-SBA-15 has proven to be a versatile catalyst for the selective oxidation with peroxide enhancement to produce fine chemicals and pharmaceuticals. To be effective, Ti should be incorporated crystallochemically in tetrahedral oxygen co-ordination (TiO_4) by isomorphic $Si^{4+} \leftrightarrow Ti^{4+}$ substitution, rather than as co-existing catalytically inactive anatase with $Ti^{4+}O_6$ octahedra [11]. Several attempts have been made to introduce titanium into the mesoporous silica framework of SBA-15 [12-18] by direct synthesis or post-synthesis treatment [9, 16, 19-23]. The principle limitation of the post-synthesis method is that metal oxides are deposited on external surfaces of the catalyst which blocks the channels and prevents the reactant molecules accessing many reactive sites in the matrix [23]. Zhang *et al.* [14] reported the successful incorporation of Ti into SBA-15 through a fluoride mediated reaction that accelerated the hydrolysis of a silica precursor. However, the expensive starting materials have limited its use. Newalkar *et al.* [16] reported the microwave-assisted hydrothermal synthesis of Ti-SBA-15 using TEOS and $TiCl_4$ as silica and titanium sources.

Wongkasemjit *et al.* [24-26] successfully prepared silatrane and titanium glycolate using inexpensive and widely available silica and titanium oxide as starting materials, respectively. The resulting moisture stable silatrane and titanium glycolate

can be effectively used to synthesize many technological materials [27-31]. Commercially available silica and titanium sources are highly susceptible to hydrolysis, resulting in the rapid separation of amorphous silica that impedes mesopore formation. Therefore, it is advantageous to use precursors of reduced hydrolytic activity. Moreover, silatrane has also been proven successful for the synthesis of SBA-15 mesoporous silica at room temperature [32]. In the present study, this approach is extended to the synthesis of highly ordered Ti-SBA-15 from silatrane and titanium glycolate precursors, where the acidity, reaction temperature, reaction time, and Ti loading were optimized systematically. The catalysts were characterized using several complimentary techniques, including SAXS, DRUV, TEM, and N_2 adsorption. The catalytic activity of Ti-SBA-15 towards the epoxidation of styrene monomers with H_2O_2 employed as the oxidant was investigated as a function of temperature, time, and catalyst loading. To establish a baseline for comparison, titanium glycolate was impregnated on a SBA-15 framework by the incipient wetness impregnation method [33].

5.3 Experimental Section

5.3.1 Materials

Fumed silica (SiO_2, 99.8%) (Sigma-Aldrich, St. Louis, MO), titanium dioxide (TiO_2) (Carlo Erba, Milan, Italy), triethanolamine (TEA) (Carlo Erba, Milan, Italy), tetraethylenetriamine (TETA) (Facai, Bangkok, Thailand), ethylene glycol (EG) (J.T. Baker, Philipsburg, NJ), acetronitrile (Labscan, Bangkok, Thailand), poly(ethylene glycol)-block-poly(propylene glycol)-block-poly(ethylene glycol) ($EO_{20}PO_{70}EO_{20}$) (Sigma-Aldrich, Singapore), hydrochloric acid (HCl) (Labscan, Asia) were used without further purification or treatment.

5.3.2 Ti-SBA-15 sol-gel synthesis

Ti-SBA-15 materials were synthesized from silatrane and titanium-glycolate. The non-ionic triblock copolymer surfactant $EO_{20}PO_{70}EO_{20}$ was used as the structure-directing agent and 2 M HCl was the acid catalyst. The preparation of Ti-SBA-15 with various n_{Ti}/n_{Si} molar ratios followed the method of Samran *et al.*

[32]. A solution of $EO_{20}PO_{70}EO_{20}$:HCl:silatrane:H_2O = 2:60:4.25:12 (mass ratio) was prepared by dissolving 4 g of $EO_{20}PO_{70}EO_{20}$ polymer in 80 g of 2 M HCl (part A) and 8.8 g of silatrane, synthesized according to ref. 25-26, in 20 g of H_2O (part B) with continuously stirring for 1 h to ensure complete dissolution. The solution of part B was then poured into part A. The required amount of titanium glycolate [24] was added into the homogenous solution with stirring. The resulting gel was aged at room temperature (RT) for 24 h and the product recovered by filtration, washed with deionized water, and dried overnight at ambient. Silicas were calcined at 550 °C in air for 6 h using a tube furnace (Carbolite, CFS 1200, Hope Valley, U.K.) at a heating rate of 0.5 °C/min to remove the residual organics. The catalysts were designated as *(x)* mol% Ti-SBA-15 where *x* denotes the percentage of the n_{Ti}/n_{Si} ratio. Titanium-free mesoporous SBA-15 was synthesized using the same procedure ($EO_{20}PO_{70}EO_{20}$:HCl:silatrane:H_2O = 2:60:4.25:12 (mass ratio)) in the absence of titanium glycolate. The reaction conditions for synthesis of Ti-SBA-15 were studied as a function of Ti loading, acidity, reaction time, and reaction temperature.

5.3.3 Ti-SBA-15 impregnation synthesis

Incipient wetness impregnation was used to deposit Ti metal on the SBA-15 support [38], using 7 and 10 mol% titanium glycolate. The precursor was dissolved in water and dropped onto the catalyst supports. Drying was carried out at 100 °C for 12 h, followed by calcination (550 °C/6 h) in a Carbolite furnace (CFS 1200) at a heating rate of 0.5 °C/min.

5.3.4 Characterization

SAXS patterns were obtained with a PANalytical PW3830 X-ray instrument using CuKα (λ_{av}=0.154 nm) radiation generated at 50kV and 40 mA, over the 2θ range 0.5–10°, step size of 0.01° and dwell time of 10 seconds per step. TEM was conducted using a JEOL JEM-2100F TEM instrument operated at an accelerating voltage of 200 kV with a large objective aperture. Nitrogen adsoption and desorption isotherms were measured at -196 °C after outgassing at 250 °C for 12 h under vacuum (Quantasorb JR, Mount Holly, NJ). The specific surface area was determined by the Brunauer–Emmett–Teller (BET) method. The pore size distributions were obtained from the adsorption and desorption branches of the

nitrogen isotherms by the Barrett-Joyner-Halenda method. DRUV spectra were recorded from 190–600 nm with a Shimadzu UV-2550 spectrophotometer from catalyst powders loaded in a teflon cell and using $BaSO_4$ as a reference.

5.3.5 Catalytic activity of Ti-SBA-15

The catalytic activity of Ti-SBA-15 towards epoxidation of styrene was established by combining 5 mmol of styrene, 5 mmol of 30% H_2O_2, 5 ml of acetronitrile and a required amount of Ti-SBA-15 (0.0500–0.2000 g) in a glass flask. The suspension was stirred and heated to a fixed time (1–6 h) and temperature (70–90 °C) in an oil bath. Chemical analyses were carried out with a gas chromatograph (GC) equipped with a capillary column (DB-Wax, 30 m x 0.25 mm) and flame ionization detector (FID). The conversion of styrene was calculated based upon the amount of styrene monomer consumed.

5.4 Results and Discussion

5.4.1 Ti-SBA-15 catalyst crystal chemistry

Zhao *et al.* [1] synthesized good quality SBA-15 of high surface area (690 m^2/g) using TEOS as the silica precursor that was aged (35 °C/20 h) prior to hydrothermal reaction (100 °C/48 h). Recently, Samran *et al.* [32] reported a novel method to prepare SBA-15 from silatrane at room temperature via a sol-gel process using a nonionic triblock copolymer as the template to avoid the need for hydrothermal treatment. Following this approach, high quality Ti-SBA-15, of large surface area (592–670 m^2/g), pore volume (0.83 cm^3/g) and pore size (5.7 nm), was readily synthesized. Generally, the SAXS pattern of SBA-15 shows scattering attributable to {10} and {30} planes of a 2D hexagonal meso-channel arrangement. These characteristic lines were also observed in Ti-SBA-15. Moreover, the nature of Ti^{4+} as substitutional TiO_4 units or extra-framework TiO_6 polyhedra could be differentiated by DRUV. Catalysts showed strong adsorption, around 220 nm, typical of the ligand-to-metal charge transfer transition in the tetrahedrally coordinated TiO_4 or $HOTiO_3$ species. This band arises from $d\pi$-$p\pi$ charge transfer between the Ti and O atoms associated with Ti-O-Si bonds and became more intense with increasing Ti

content. An additional band at 330 nm for higher Ti contents is attributed to extra-framework titanium (probably anatase), suggesting there is an upper limit for Ti displacement of Si in the SBA-15 framework [34].

5.4.2 Effect of Ti loading

The SAXS patterns of calcined Ti-SBA-15 with 1-10 mol% Ti loading all show intense {10} ≡ {11} and {30} ≡ {33} reflections associated with *p6mm* plane symmetry [32] indicative of well ordered mesopores (Figure 1A). As Ti loading increased SBA-15 was not perturbed, due to the mild synthesis conditions and extraordinarily high purity and moisture stability of the silatrane precursor. TEM of the Ti-SBA-15 (7 mol% Ti loading) directly confirmed the long range periodicity of the mesopores [2] (Figure 2). N_2 adsorption/desorption isotherms and pore size distribution patterns provide quantitative assessments of the porosity (Figure 3). All catalysts yielded a type IV isotherm (IUPAC classification), with a H1 type hysteresis loop characteristic of a large diameter mesoporous solid with narrow pore size distribution [2]. The well-defined step at a relatively high pressure of 0.5–0.7 corresponds to capillary condensation of N_2, within uniform pores (> 5 nm diameter) and surface area (up to 670 m^2/g) (Table 1). The BET surface area and pore size slightly decrease with increasing Ti loading. DRUV spectra of Ti-SBA-15 all show an absorption band centered at ~ 220 nm, with the intensity increasing with Ti loading (Figure4A), that is attributed to charge transfer transition associated with isolated $Ti^{4+}O_4$ coordination. However, at the 10%mol Ti loading, the 330 nm band appears from extra-framework anatase $Ti^{4+}O_6$.

5.4.3 Effect of acidity

The SAXS patterns of Ti-SBA-15 materials prepared at different acidity are shown in Figure 1B, all exhibit a clear {10} reflection indicating uniform pore diameter, but the {30} reflection is broad when the acidity is reduced to 1M, suggesting that interpore order correlation is limited. Additionally, DRUV showed strong absorption at 220 nm for the 1M HCl sample as direct evidence for Ti^{4+} incorporated into the mesoporous silica framework (Figure 4B). It can be concluded that lower acidity favored framework incorporation of Ti which disrupts long range order in SBA-15 in agreement with Vinu *et al.* [12], who reported that lowering the

acidity decreases the hydrolysis rate of the titanium precursors to match that of silica precursors. This may enhance the interaction between the Ti-OH and Si-OH species in the gel resulting in more complete Ti incorporation. At the highest acid concentration (3M HCl), DRUV yielded weak absorption at 220 nm, due to the ready dissociation of Ti-O-Si bonds [13]. While a change in acid concentration does not notably affect the surface area, pore volume and pore size (Table 2), the use of 2 M HCl is considered optimal because it maintained the well ordered structure of the mesopores and showed high Ti incorporation.

5.4.4 Effect of temperature

Temperature affects liquid crystal formation [30]. In the present case, increasing the reaction temperature from ambient to 80 °C for Ti-SBA-15 catalyst (10mol% Ti loading/2M HCl/24 h) showed {10} periodicity remained intact while {30} was absent (Figure 1C). BET confirmed the increase in pore size with reaction temperature (Table 3), while DRUV showed that at 80 °C, $Ti^{4+}O_6$ disappeared because the Ti^{4+} species preferentially displaced Si^{4+} in the framework of SBA-15 (Figure 4C). However, 2D order was compromised at the higher temperature, and therefore room temperature proved most suitable for the synthesis of Ti-SBA-15. Zhao *et al.* [2] reported that higher temperatures resulted in larger pore sizes possibly due to the PEO blocks becoming more hydrophobic that increased hydrophobic domain volumes, and lead to wider channels with accelerated Ti^{4+} incorporation into the SBA-15 framework but simultaneously limited long range order.

5.4.5 Effect of aging time

Aging time is an important parameter because in alkoxide-derived gels, the condensation reaction between surface functional groups continues beyond the gel point. During aging, there are changes in the textural and physical properties of the gel, and from 12 to 36 h (10mol% Ti loading/2 M HCl / RT) SAXS revealed that whilst the narrow {10} reflection is preserved, the {30} reflection broadens with aging time due to disruption of long-range hexagonal periodicity [30] (Figure 1D). DRUV spectra indicate that with longer aging extra framework anatase $Ti^{4+}O_6$ appears (Figure 4D), while N_2 adsorption isotherms found the surface area, pore volume and pore size all decreased (Table 4). It is believed that long reaction times,

beyond equilibrium, cause the condensation reaction to reverse, resulting in mesopore deterioration [35].

5.4.6 Catalytic activity of Ti-SBA-15 towards styrene epoxidation

Styrene oxide and benzaldehyde were the principle products of styrene epoxidation with H_2O_2 over Ti-SBA-15. All titanium loaded catalysts demonstrated considerably higher styrene conversion than pure SBA-15 (Table 5). Raising the Ti content to 7 mol% increased the conversion of styrene remarkably (from 2.9% to 25.8%) with the selectivities for styrene oxide and benzaldehyde of 34.2% and 65.8%, respectively. Additionally, Ti-SBA-15 prepared by the sol-gel synthesis showed significantly higher conversion of styrene (25.8%) than an equivalent catalyst (in terms of Ti content) synthesized by the impregnation method (11.9%). When Ti content exceeds 7 mol% conversion efficiency decreases (from 25.8% to 12.4%), in agreement with DRUV that found the $Ti^{4+}O_4$ content was maximized in this catalyst beyond which $Ti^{4+}O_6$ extra-framework titanium appears as anatase which is less active. Combined with the diffraction and microscopy results, it is confirmed that Ti^{4+} incorporated within the SBA-15 framework is most active. This conclusion is consistent with Zhang *et al.* [14] and Ji *et al.* [36], who reported that the titanium species in the SBA-15 framework are the active sites for styrene oxidation reaction. Moreover, the selectivity of styrene oxide decreased while selectivity of benzaldehyde increased with titanium loading consistent with the study of Yu *et al.* [37] who reported that an increase of the Ti content in the mesoporous catalysts decreases epoxide selectivity and H_2O_2 efficiency due to a decrease of isolated Ti atoms in the SBA-framework.

Figure 5A shows that over 7 mol% Ti-SBA-15 styrene conversion increases with time whereas selectivity decreases, which may attributed to the secondary oxidation of styrene oxide [33]. The reaction is initially rapid due to the abundance of H_2O_2 [36], reaches a maximum after 4 h, then remains constant for up to 6 h. The conversion of styrene slightly increased by raising the temperature from 70 to 90 °C (Figure 5B) consistent with the study of Laha *et al.* [38], but the selectivity of Ti-SBA-15 toward styrene oxide was highest at 80 °C. The selectivity of benzaldehyde also increased with increasing the reaction temperature, meaning

that the higher temperature favors further oxidation of styrene oxide [11]. The effect of catalyst concentration is shown in Figure 5C, with styrene conversion increasing from 11.2% to 25.8% as the mass of catalyst was adjusted from 0.05 g to 0.10 g, beyond which the rate was essentially constant. The initial improvement in performance with catalyst loading is due to an increase of active Ti sites in the system that facilitates styrene conversion [38].

5.5 Conclusions

Ti-SBA-15 was successfully synthesized via a sol-gel process using silatrane as the silica precursor, titanium glycolate as a titanium source, and nonionic triblock copolymer as a template. The method is straightforward and can be conducted at room temperature without the need for hydrothermal treatment as conventionally required. Systematic variations of acidity, aging temperature, aging time, and Ti loading lead to an optimized Ti-SBA-15 product. Crystallochemical incorporation of titanium by $Ti^{4+}O_4$ substitution for $Si^{4+}O_4$ in the mesopores proves superior to impregnation or decoration with anatase ($Ti^{4+}O_6$). Tetrahedral Ti^{4+} coordination is maintained to a loading of 7 mol% titanium. Ti-SBA-15 materials show relatively high activity in the epoxidation reaction of styrene monomers due to the presence of $Ti^{4+}O_4$ in the SBA-15 framework. For the optimized catalyst (7 mol% Ti loading/2 M HCl/24 h/RT), the epoxidation reaction of styrene was most effective at 80 °C/4 h, using 0.05 g catalyst with the only products being styrene oxide and benzaldehyde. The selectivity of styrene oxide and benzaldehyde reached 34.2% and 65.8% at a styrene conversion of 25.8%. This research demonstrates that Ti-SBA-15 heterocatalyst can be synthesized by a low cost and energy efficient process that will allow scale-up for possible industrially application.

5.6 Acknowledgements

This research work is financially supported by the Postgraduate Education and Research Program in Petroleum and Petrochemical Technology (ADB) Fund (Thailand), the Ratchadapisake Sompote Fund, Chulalongkorn University, and the

Thailand Research Fund (TRF). The SAXS patterns were collected by Mr. An Tao and Ms. Li Henan at the School of Materials Science and Engineering, Nanyang Technological University.

5.7 References

1. Zhao, D.; Feng, J.; Huo, Q.; Melosh, N.; Frerickson, G. H.; Chmelka, B. F.; Stucky, G. D. *Science* **1998**, *279*, 548-552.
2. Zhao, D.; Huo, Q.; Feng, J.; Chmelka, B. F.; Stucky, G. D. *J. Am. Chem. Soc.* **1998**, *120*, 6024-6036.
3. Sayari, A. *Chem Mater.* **1996**, *8*, 1840.
4. Corma, A. *Chem. Rev.* **1997**, *97*, 2373.
5. Soler-Illia Galo, J. De A.A.; Sanchez, C.; Lebeau, B.; Patarin, J. *Chem. Rev.* **2002**, *102*, 4093.
6. Taguchi, A.; Schuth, F. *Micropor. Mesopor. Mater.* **2005**, *77*, 1.
7. He, N.; Bao, S.; Xu, Q. *Appl. Catal.: A* **1998**, *169*, 29.
8. Corma, A.; Fornes V.; Navarro, M.T.; Perez-Pariente, J. *J. Catal.* **1994**,*148*, 569.
9. Vinu, A.; Murugesan, V.; Bohlmann, W.; Hartmann, M. *J. Phys. Chem. B* **2004,** *108,* 11496.
10. Vinu, A.; Murugesan, V.; Tangermann, O.; Hartmann, M. *Chem. Mater.* **2004,** *16*, 3056.
11. Wu, P.; Tatsumi, T. *Chem. Mater.* **2002**, *14*, 1657-1664.
12. Vinu, A.; Srinivasu, P.; Miyahara, M.; Ariga, K. *J. Phys. Chem. B* **2006**, *110*, 801-806.
13. Chen, Y.; Huang, Y.; Xiu, J.; Han, X.; Bao, X. *Appl. Catal. A: Gen.* **2004**, *273*, 185.
14. Zhang, W. H.; Lu, J.; Han, B.; Li, M.; Xiu, J.; Ying, P.; Li, C. *Chem. Mater.* **2002**, *14*, 3413.
15. Wu, S.; Han, Y.; Zou, Y. C.; Song, J. W.; Zhao, L.; Di, Y.; Liu, S. Z.; Xiao, F. S. *Chem. Mater.* **2004**, *16*, 486.
16. Newalkar, B. L.; Olanrewaju, J.; Komarneni, S. *Chem. Mater.* **2001**, *13*, 552.
17. Berube, F.; Kleitz, F.; Kaliaguine, S. *J. Phys. Chem. C* **2008**, *112*, 14403.

18. Berube, F.; Kleitz, F.; Kaliaguine, S. *J. Mater. Sci.* **2009**, *44*, 6727.
19. Luan, Z. H.; Hartmann, M.; Zhao, D. Y.; Zhou, W. Z.; Kevan, L. *Chem. Mater.* **1999**, *11*, 1621.
20. Luan, Z. H.; Bae, J. Y.; Kevan, L. *Chem. Mater.* **2000**, *12*, 3202.
21. Morey, M. S.; O'Brien, S.; Schwarz, S.; Stucky, G. D. *Chem. Mater.* **2000**, *12*, 898.
22. Yue, Y. H.; Gedeon, A.; Bonardet, J. L.; Melosh, N.; D'Espinose, J. B.; Fraissard, J. *Chem. Commun.* **1999**, 1967.
23. Murugavel, R.; Roesky, H. W. *Angew. Chem., Int. Ed. Engl.* **1997**, *36*, 477.
24. Phonthammachai, N.; Chairassameewong, T.; Gulari, E.; Jamieson, A.M.; Wongkasemjit, S. *Met. Mater. Min.* **2002**, *12*, 23-28.
25. Phiriyawirut, P.; Magaraphan, R.; Jamieson, A. M.; Wongkasemjit, S. *Material Science and Engineering A* **2003**, *361*, 147-154.
26. Charoenpinijkarn, W.; Suwankruhasn, M.; Kesapabutr, B.; Wongkasemjit, S.; Jamieson, A. M. *European Polymer Journal* **2001**, *37*, 1441-1448.
27. Phonthammachai, N.; Chairassameewong, T.; Gulari, E.; Jemieson, A.M.; Wongksemjit, S. *Microporous and Mesoporous Material* **2003**, *66*, 261-271.
28. Tanglumlert, W.; Imae, T.; White, T. J.; Wongkasemjit, S. *Materials Letters* **2008**, *62*, 4545-4548.
29. Sathupanya, M.; Gulari, E.; Wongkasemjit, S. *J. Eur. Ceram. Soc.* **2003**, *23*, 2305–2314.
30. Phiriyawirut, P.; Jamieson, A. M.; Wongkasemjit, S. *Microporous Mesoporous Mater.* **2005**, *77*, 203–213.
31. Thanabodeekij, N.; Sadthayanon, S.; Gulari, E.; Wongkasemjit, S. *Mater. Chem. Phys.* **2006**, *98*, 131–137.
32. Samran, B.; White, T.J.; Wongkasemjit, S. *Journal of Porous Materials* **2010** DOI. 10.1007/s10934-010-9367-3
33. Tanglumlert, W.; Imae, T.; White, T. J.; Wongkasemjit, S. *Cat. Comm.* **2009**, *10*, 1070-1073.
34. Wang, Y.; Zhang, Q.; Shishido, T.; Takehira, K. *J. Catal.* **2002**, *209*,186-196.
35. Yilmaz, VT.; Topcu, Y.; Karadag A. *Thermchimica Acta* **2002**, *383*, 129-133.

36. Ji, D.; Zhao, R.; Lv, G.; Qian, G.; Yan, L.; Suo, J. *Applied Catalysis A : General* **2005**, *281*, 39-45
37. Yu, J.; Feng, Z.; Xu, L.; Li, M.; Xin, Q.; Liu, Z.; Li, C. *Chem. Mater.* **2001**, *13*, 994.
38. Laha, S.C.; Kumar, R. *J. of catal.* **2001**, *204*, 64-70.

Table 1. BET and SAXS analyses of Ti-SBA-15 as a function of amount of Ti loading

Loaded Ti (%)	Surface area (m^2/g)	Pore Volume (cm^3/g)	Channel diameter (nm)	
	BET	BET	BET	SAXS
1	670	0.83	5.79	6.8
3	643	0.81	5.77	6.7
5	618	0.76	5.40	6.5
7	592	0.67	5.39	6.5
10	597	0.71	5.37	6.4

Table 2. BET and SAXS analyses of Ti-SBA-15 as a function of acidity

Acidity (M)	Surface area (m^2/g)	Pore Volume (cm^3/g)	Channel diameter (nm)	
	BET	BET	BET	SAXS
1 M	582	0.78	5.63	-
2 M	597	0.71	5.37	6.4
3 M	606	0.74	5.38	6.2

Table 3. BET and SAXS analyses of Ti-SBA-15 as a function of temperature

Temperature (°C)	Surface area (m^2/g)	Pore Volume (cm^3/g)	Channel diameter (nm)	
	BET	BET	BET	SAXS
RT	597	0.71	5.37	6.4
50	596	0.72	5.68	-
80	626	0.95	6.60	-

Table 4. BET and SAXS analyses of Ti-SBA-15 as a function of aging time

Time (h)	Surface area (m^2/g)	Pore Volume (cm^3/g)	Channel diameter (nm)	
	BET	BET	BET	SAXS
12	637	0.79	5.68	6.4
24	597	0.71	5.37	6.4
36	609	0.71	5.39	-

Table 5. Comparison of catalysts for epoxidation of styrene

Catalyst (%)	Styrene conversion (%)	Selectivity (%)	
		Styrene oxide	Benzaldehyde
0% Ti (sol-gel)	2.9	46.6	53.4
3% Ti (sol-gel)	14.4	42.1	57.9
5% Ti (sol-gel)	13.9	36.8	63.2
7% Ti (sol-gel)	25.8	34.2	65.8
10% Ti (sol-gel)	12.4	30.1	69.9
7% Ti (impreg.)	11.9	45.7	54.3
10% Ti (impreg.)	10.2	29.2	70.8

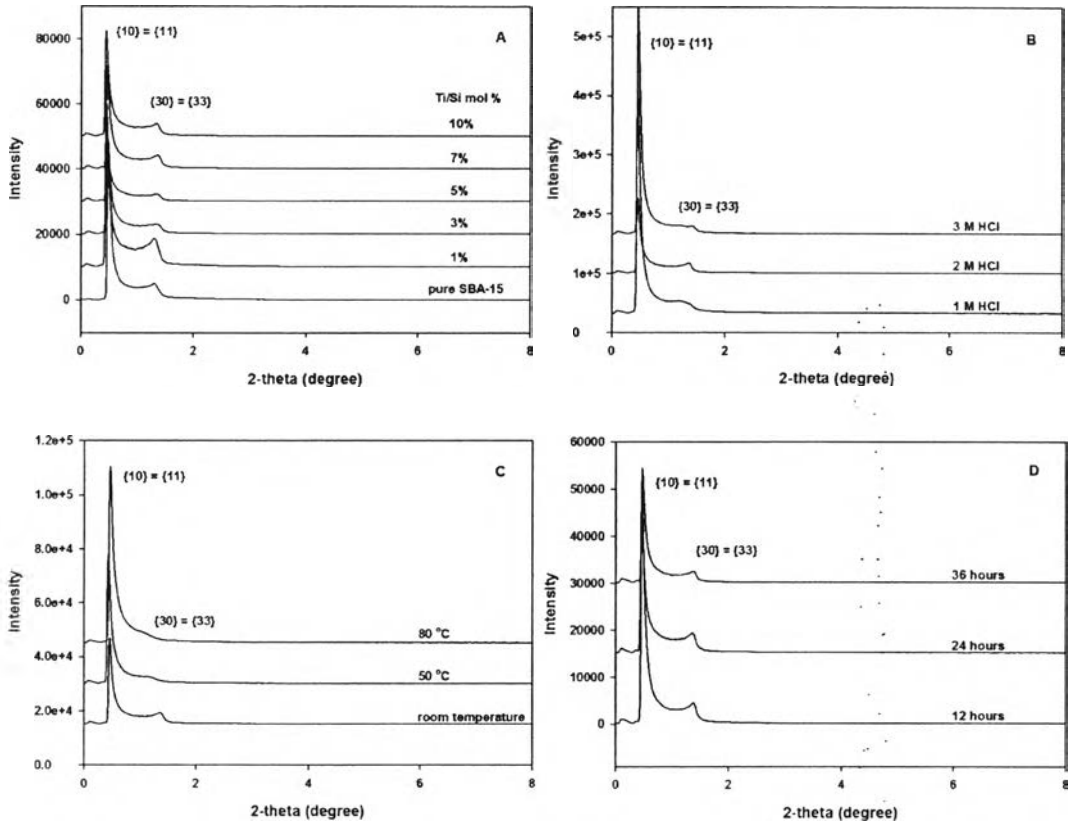

Figure 1 SAXS patterns of (A) pure silica SBA-15 and Ti-incorporated samples of Ti-SBA-15 containing different amount of Ti loadings; (B) Ti-SBA-15 materials prepared at different acid concentrations; (C) Ti-SBA-15 synthesized at different temperatures; (D) Ti-SBA-15 synthesized at different aging times.

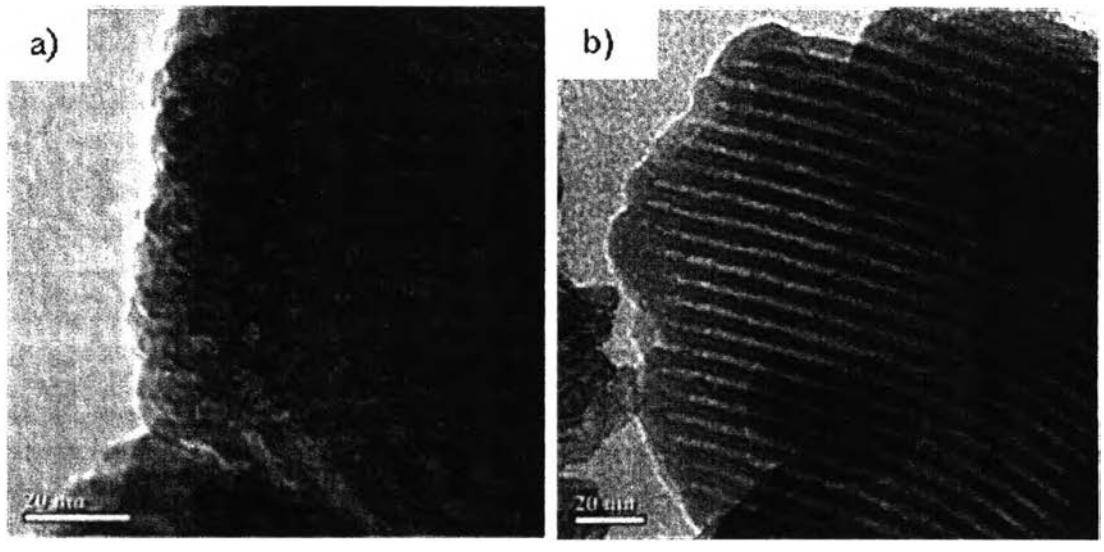

Figure 2 TEM images of 7 mol% Ti-SBA-15, in which a) in the direction perpendicular to the pore axis and b) in the direction parallel to the pore axis.

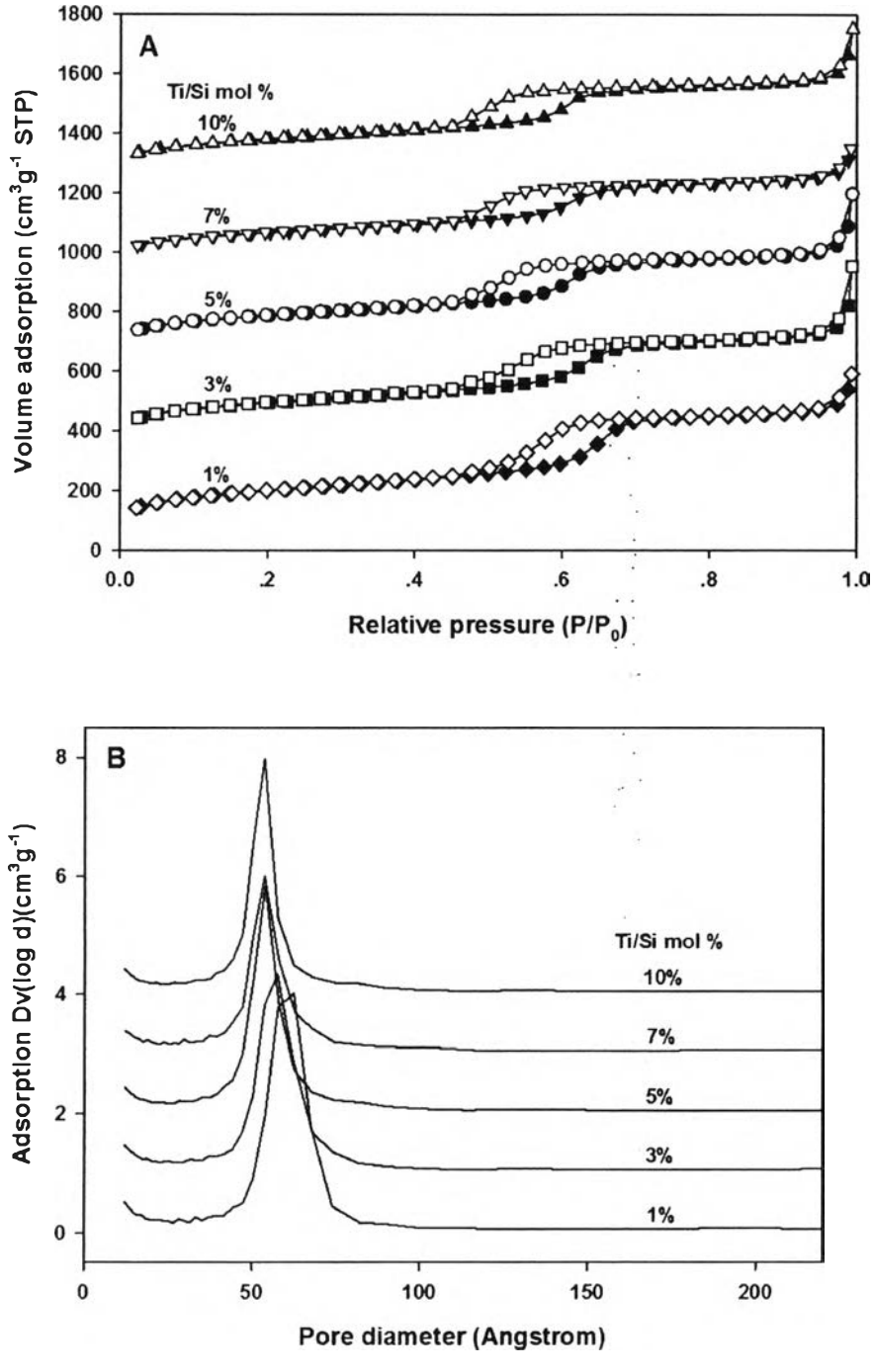

Figure 3 N_2 adsorption/desorption isotherms (A) and pore size distributions (B) of Ti-SBA-15 containing different amount of Ti loadings.

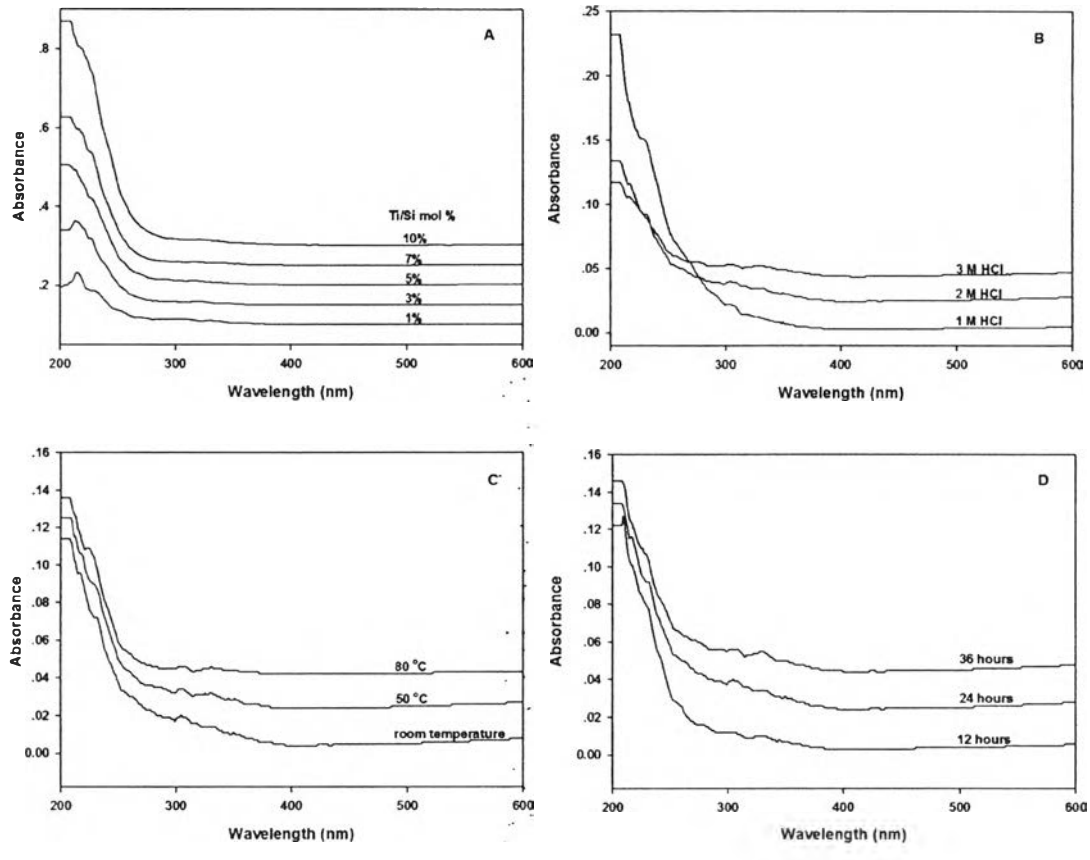

Figure 4 Diffuse reflectance UV-visible spectra of the synthesized Ti-SBA-15: (A) at different amounts of Ti loadings; (B) at various acid concentrations; (C) at different temperatures; and (D) at different aging times.

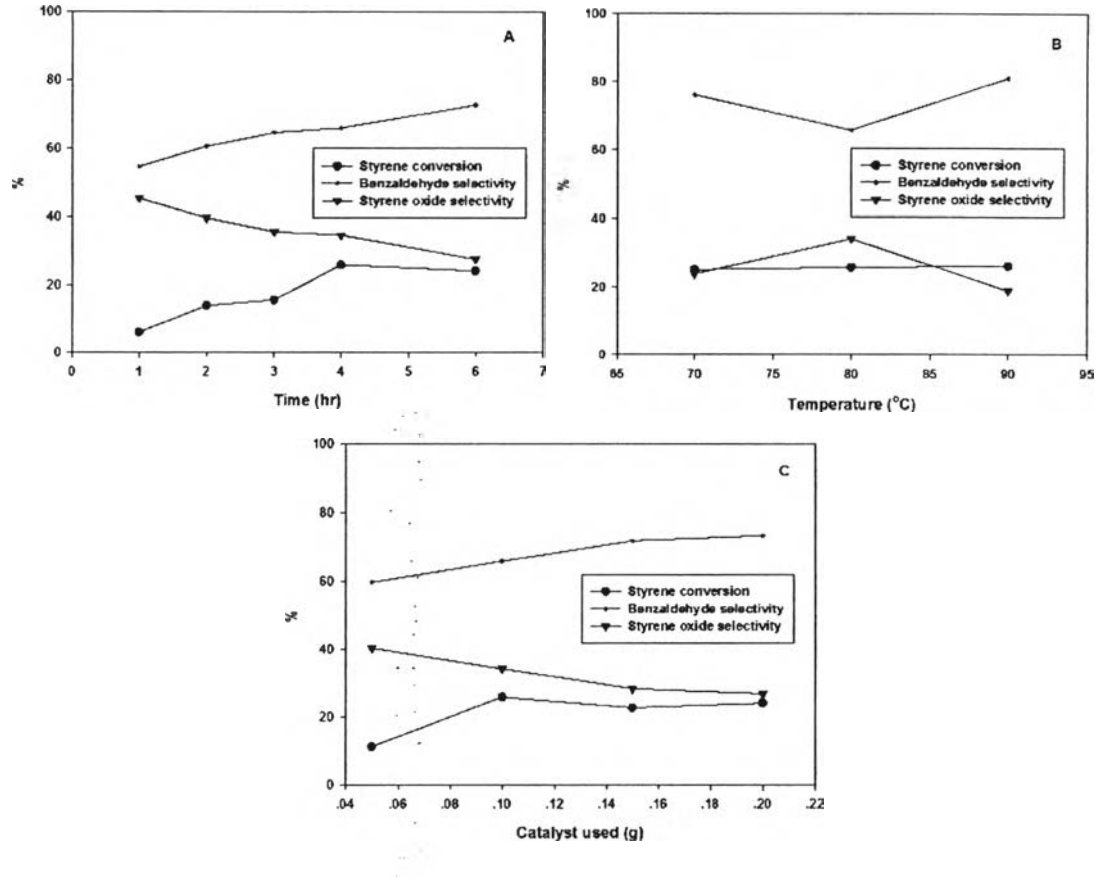

Figure 5 (A) Effect of reaction time on the styrene oxidation using 0.1 g of catalyst, containing 7.0 mol% titanium content, at 80 °C; (B) Effect of reaction temperature on the styrene oxidation using 0.1 g of catalyst, containing 7 mol% titanium content, for 4 h; (D) Effect of amount of catalyst, containing 7.0 mol% titanium content, at 80 °C for 4 h.